Langmuir

Article

pubs.acs.org/Langmuir

Structure of Water at Charged Interfaces: A Molecular Dynamics Study

Shalaka Dewan,[†] Vincenzo Carnevale,[‡] Arindam Bankura,[‡] Ali Eftekhari-Bafrooei,[†] Giacomo Fiorin,[‡] Michael L. Klein,[†,‡] and Eric Borguet*[,†]

[†]Department of Chemistry, Temple University, Philadelphia, Pennsylvania 19122, United States

[‡]Institute for Computational Molecular Science, Temple University, Philadelphia, Pennsylvania 19122, United States

ABSTRACT: The properties of water molecules located close to an interface deviate significantly from those observed in the homogeneous bulk liquid. The length scale over which this structural perturbation persists (the so-called interfacial depth) is the object of extensive investigations. The situation is particularly complicated in the presence of surface charges that can induce long-range orientational ordering of water molecules, which in turn dictate diverse processes, such as mineral dissolution, heterogeneous catalysis, and membrane chemistry. To characterize the fundamental properties of interfacial water, we performed molecular dynamics (MD) simulations on alkali chloride solutions in the presence of two types of idealized charged surfaces: one with the charge density localized at discrete sites and the other with a homogeneously distributed charge density. We find that, in addition to a diffuse region where water orientation shows no layering, the interface region consists of a "compact layer" of solvent next to the surface that is not described in classical electric double layer theories. The depth of the diffuse solvent layer is sensitive to the type of charge distributions on the surface and the ionic strength. Simulations of the aqueous interface of a realistic model of negatively charged amorphous silica show that the water orientation and the distribution of ions strongly depend on the identity of the cations (Na^+ vs Cs^+) and are not well represented by a simplistic homogeneous charge distribution model. While the compact layer shows different solvent net orientation and depth for Na^+ vs Cs^+, the depth (~1 nm) of the diffuse layer of oriented waters is independent of the identity of the cation screening the charge. The details of interfacial water orientation revealed here go beyond the traditionally used double and triple layer models and provide a microscopic picture of the aqueous/mineral interface that complements recent surface specific experimental studies.

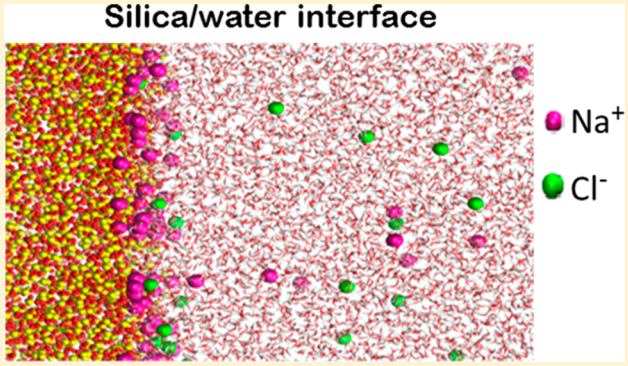

INTRODUCTION

The unique properties of interfacial water impact diverse fields such as biology[1−3] (e.g., protein folding and lipid membrane properties), geology[4,5] (e.g., mineral dissolution, the stability of colloids, and wastewater treatment), atmospheric chemistry[6] (e.g., effect of water aerosols on pollution), electrochemistry[7] (e.g., wetting and corrosion), materials science[8] (e.g., heterogeneous catalysis), and technological applications[9] (e.g., hydrogen fuel cells and biosensors). Despite the profound differences in the physicochemical processes involved in the above examples, they all depend on the interaction of water molecules with surfaces and the influence of the surface on the structure of the extended hydrogen bond network.[10] Water molecules at interfaces have different properties than their bulk counterparts[11,12] due to the abrupt break in the bulk hydrogen-bonding network caused by the presence of a phase boundary. It is this peculiar orientation and ordering of the first layer of water molecules at the interface that influence many macroscopic interfacial processes.[11,13]

At the well-studied air/water interface, experimental and theoretical results show that the interfacial depth, i.e., the region where the water structure is not bulklike, is rather shallow (~3−7 Å), corresponding to one or two monolayers.[14,15] A different picture is expected at mineral/water or electrode/electrolyte interfaces, where surface charge may be the main factor influencing the local hydrogen-bonding environment of water. In particular, the region that is inherently oriented due to the presence of the surface may extend well beyond the first layer.[16−18] The surface charge induces an electrostatic field that can align water molecules, inducing an orientational order that persists over a certain depth into the bulk, as described by simple electrostatic models[10] and confirmed experimentally.[19−21]

In the presence of electrolytes, the surface charge is balanced by the distribution of counterions and oriented water dipoles near the interface, forming an electric double layer (EDL) region, our understanding of which has been ever-evolving since the early introduction of classical theoretical models.[22,23]

Received: March 23, 2014
Revised: June 5, 2014
Published: June 30, 2014

   dx.doi.org/10.1021/la5011055 | *Langmuir* 2014, 30, 8056−8065

The commonly adopted, and so far experimentally consistent, model is the Gouy−Chapman−Stern (GCS) or modified Gouy−Chapman model.[23] According to this model, the surface charge balance is established by specific adsorption of ions to and orientation of solvent molecules at the so-called inner Helmholtz plane. This is followed by nonspecific adsorption of hydrated counterions at the outer Helmholtz plane. These planes together form the compact Stern layer. Additional nonspecifically adsorbed ions are distributed in the "diffuse layer", a region where the concentration of ions gradual decays toward the bulk. These three components are the major constituents of the GCS model.[10,23,24] While this model accurately predicts the long-range behavior of the charge distribution, it fails to provide a reliable description in the region close to the surface as it neglects ion−ion correlations.[22,24]

Surface-specific experimental techniques, such as second harmonic generation (SHG) and vibrational sum-frequency generation (vSFG),[25] that are sensitive to inhomogeneous structures have shown that surface charge (determined by pH at mineral surfaces) strongly orients water close to the surface and that addition of salt significantly perturbs this orientational ordering.[26−28] Heterodyne vSFG measurements have further confirmed that water molecules at a surfactant boundary orient themselves with their hydrogens pointing up when the surfactant is negatively charged and exhibit "flip-flop orientation", as the surface charge is switched from negative to positive.[19,21] However, in addition to probing surface structure, many of these surface-specific experimental techniques are also sensitive to the effective electric field induced at a surface. In fact, based on recent vibrational SFG dynamics and SHG experiments of water at silica surfaces,[26,29] it was hypothesized that cations accumulate at negatively charged surfaces and screen the electric field such that the depth of surface-field ordered water is much smaller than that predicted by Gouy−Chapman theory.[26] As a result, it is difficult to separate structural changes in the interfacial solvent layer from changes in the effective interfacial electric field, and the detailed structure of water layers very close to the surface remains ambiguous. Simulation studies can provide such details and have been useful in testing the validity of classical electrochemical models and experimental interpretation.[24,30,31]

Molecular dynamics (MD) simulations are particularly suitable for addressing the detailed interfacial aqueous structure at charged surfaces, as they can explicitly provide a microscopic description of the system.[16,22,32] The numerous MD simulations of solid/aqueous interfaces have clarified some important behavioral properties of interfacial water. For example, water at flat hydrophobic surfaces shows orientational ordering which is *inverted* with respect to that observed for small hydrophobic solutes.[33] Further, by increasing the hydrophilicity of the surface, the preferential orientation of interfacial water within 3 Å from the surface was shown to completely switch direction.[34] Likewise, in going from a hydrophobic graphite surface to a SiO_2 surface with a high density of hydroxyl groups, the extent of orientational ordering induced in the first two layers increased significantly.[35]

MD simulations of water at a metallic electrode surface with constant potential presented by Willard et al. show that water ordering close to the surface is quite different from what is predicted by continuum models.[16] At this surface, the adsorption of ions is strongly inhibited by the presence of an adsorbed water layer, independent of the electrode potential.[16] *Ab initio* MD simulations of water flow dynamics at silica surface reiterate the limitation of the Stern model in satisfactorily describing a region of gradually reduced water mobility adjacent to the surface.[36] In the case of salt solutions inside positively-charged silica nanopores, ion-specific behavior of NaCl and CsCl, unaccounted for in GSC model, has been reported where Na^+ ions showed different adsorption behavior than Cs^+.[37,38] Further, at a negatively charged clay surface, the structure and dynamics of water were reported to be perturbed up to a depth of three layers of water without any effect of the nature of the counterion.[39] While these reports have contributed tremendously in developing a better picture of interfacial water, fundamental questions such as "how deep is the interfacial layer of water oriented at a mineral surface?", "how does the nature of the interfacial charge distribution affect solvent structure?", and "how does the identity of ions change water orientation?" still remain to be answered.

We have attempted to answer these questions with a molecular level investigation of the structure of an aqueous electrolyte near a charged surface using classical MD simulations for two types of surfaces with varying charge distributions. An idealized hard wall surface with no crystalline structure was chosen to eliminate any lattice-dependent solvent structuring along the *XY* direction and enable a simplified analysis of water orientation. Two strikingly different pictures emerge for the interfacial solvent region depending on whether the surface charge is localized or homogeneously spread. These results help rationalize the subsequent simulations carried out on the more realistic models of charged silica in the presence of NaCl and CsCl. Anticipating our results, we find that the NaCl/silica interface is well represented by a surface that has localized charge centers whereas the CsCl/silica interface behaves close to an interface with homogeneous charge distribution, suggesting a strong dependence of water orientation on the identity of the cation.

METHODS

Simulations were performed using the CHARMM27 force field.[40,41] The water molecules were described using the TIP3P model.[42,43] Periodic boundary conditions were employed in each spatial direction, and the electrostatic potential was evaluated using the particle-mesh Ewald method with a mesh size of 0.5 Å.[44] A cutoff of 12 Å was used for nonbonded interactions. The system was maintained at a temperature of 300 K and pressure of 1 atm using the Langevin thermostat and barostat methods as implemented in the MD code NAMD2.8 (the area of the surface is kept constant, while the size of the box is allowed to fluctuate in the orthogonal direction).[45] The idealized surface was modeled as a single layer of particles arranged in a two-dimensional lattice, with a lattice spacing of 0.5 Å, interacting with waters and ions through Lennard-Jones and electrostatic interactions. Specifically, each particle was treated as a carbon atom using, for the C_{12} and C_6 coefficients, the CHARMM-36 force-field parameters. Standard mixing rules were used to treat Lennard-Jones cross-interactions. In the case of the localized charge, particles were randomly selected and assigned a unitary amount of negative charge. The initial configuration and parameters for the amorphous silica system were taken from Cruz-Chu et al.[46] The idealized surface/water systems (both localized and homogeneously distributed charge) were built by adding 19515 water molecules, and the amorphous silica/water system had 25204 water molecules, making a water slab of approximately 250 Å. Ionic strengths of 0.1, 0.35, and 0.5 M were considered by adding the appropriate ion pairs. All the systems studied have an overall charge neutral state. The negative surface charge is compensated by adding extra counterions (Na^+ or Cs^+). Equations of motion were integrated using a time step of 2.0 fs. Each trajectory was collected for a total simulated time of 100 ns. Analysis was performed

dx.doi.org/10.1021/la5011055 | *Langmuir* 2014, 30, 8056−8065

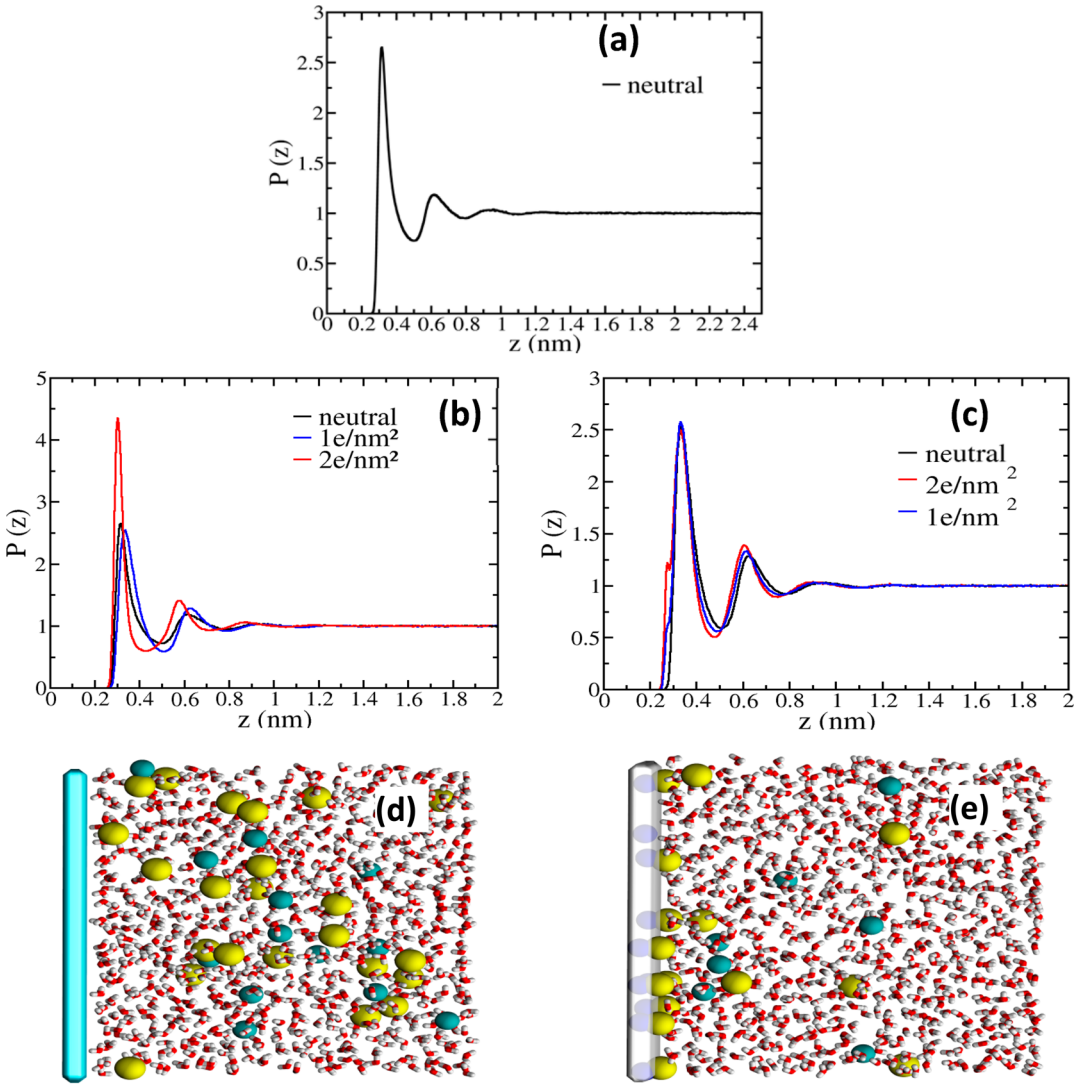

Figure 1. Density profiles of oxygen as a function of distance from an idealized surface with (a) zero-charge and ion-free water, (b) homogeneously spread charge with 0.5 M NaCl, and (c) localized charge with 0.5 M NaCl. Bottom panel: snapshots of the simulation box with 0.5 M NaCl, (d) surface with homogeneously distributed charge indicated by blue shading, and (e) localized charge at random points represented by shaded points on the surface; yellow spheres: Na ions; blue spheres: Cl ions. Mass densities (kg/m^3) were rescaled to get an asymptotic (bulk) value of 1, except where otherwise specified.

using the computational tools *g_density* and *g_order* from the GROMACS package. To quantify orientational ordering, we plot $\langle\cos(\theta)\rangle$, the average cosine of the angle between the opposite of the permanent dipole moment (Figure 3 a inset) of each water molecule and the surface normal, as a function of distance from surface.

RESULTS AND DISCUSSION

Structure of Water at Idealized Surface. Even at zero charge, the density profile of the water oxygen (Figure 1a) shows that, at the interface, water deviates from its bulk average density value. At least three distinct peaks appear, suggesting a "layering" that extends up to ∼1.2 nm from the surface, consistent with several previous MD studies.[47,48] To explore the effect of surface charge magnitude and ionic concentration on water orientation and salt distribution, we modeled the surface in two alternative simplified scenarios: with either a diffuse or localized charge density (Figure 1b−e).

Translational Order at Spread versus Localized Charge. While the number of layers is not significantly different for these two types of surface charge distributions (Figure 1b,c), we observe a different response to the increasing surface charge for the two cases. In both cases, and similar to a neutral surface (Figure 1a), the deviation from the average density extends up to three layers of water molecules from the surface and is independent of the magnitude of the charge density (1 or 2 e/nm^2) (Figure 1b,c). The short-range ordering at the homogeneous-charge surface, however, is increased at higher charge magnitude, as reflected by the increased height and slight shift of the first peak toward the surface of the density distribution function (Figure 1b). The subsequent layers of water (second peak and minima) are also shifted with increasing surface charge, albeit to a smaller extent.

In contrast, when the surface charged is localized, the short-range ordering appears largely insensitive to the magnitude of surface charge (Figure 1c). An interesting observation, however, is the shoulder-like feature or high oxygen density before the first maxima, which could corresponds to a thin layer of adsorbed water molecules or waters of the hydration shell of Na^+ ions. The density of this adsorbed layer, absent at the

dx.doi.org/10.1021/la5011055 | *Langmuir* 2014, 30, 8056−8065

homogeneous charge surface, increases with surface charge or when more cations are driven to the surface. In general, the type of charge distribution and the magnitude of surface charge does not alter the depth of ∼1.2 nm, into which water exhibits layering structure.

Distribution of Ions at Two Surfaces. The limitation of the Gouy−Chapman−Stern model in providing a detailed structure of the ions in proximity of the surface is demonstrated by our results on the distribution of cations near the surface with homogeneously spread charge (Figure 2). Within 1 nm from the surface, there is a significantly greater accumulation of cations at the surface than that predicted by the GCS model (Figure 2a−c).[23,24] Interestingly, the homogeneously charged surface shows the first water density peak closer to the surface than the first peak of the cation density, indicating that cations do not bind the surface directly (Figure 2a). Additionally, there are at least two well-defined layers of solvated Na^+. The depletion of Cl^- anions close to the surface and the long-range exponential decay of Na ions before eventually matching the bulk density (Figure 2a) are both consistent with the Gouy−Chapman prediction. When the surface charge is localized (Figure 2b,c), the distribution of cations and anions is significantly different and strongly depends on the ionic strength. First, irrespective of the ionic strength, there is an increased density of cations very close to the surface before the first maxima of density of water, indicating specific adsorption of cations without their complete hydration shells (Figure 2b,c). Second, increasing the ionic strength from 0.1 to 0.5 M NaCl causes a depletion of cations from the two solvated layers and an increase in the relative abundance of anions (Figure 2c). This result is especially remarkable as it suggests that, beyond a critical concentration, anions start to play a role in determining the water structure close to a negatively charged surface, an observation that is beyond the scope of the Gouy−Chapman−Stern model.[23,24] The following results on the two types of surfaces will show that it is the extent of cation adsorption, more than the magnitude of the charge density on the surface, that influences the interfacial water structure and orientation.

Orientational Order: Effect of Charge. In addition to causing translational ordering, as reflected by the oxygen density profiles (Figure 1a−c), the electric fields induce some "orientational ordering", as represented by the nonzero value of the $\langle\cos(\theta)\rangle$, as a function of distance from the surface (note that in a perfectly isotropic environment, e.g., bulk water, $\langle\cos(\theta)\rangle$ is zero) (Figure 3). A $\langle\cos(\theta)\rangle$ value of −1 represents a situation where all of the waters are oriented with their hydrogen pointing toward the surface. As expected, at zero charge (neutral) surface (Figure 3a,b), there is no orientational preference for water molecules, even very close to the surface, as indicated by the almost-zero value of $\langle\cos(\theta)\rangle$.

Interestingly, when a charge magnitude of 1 or 2 e/nm^2 is applied on the surface, the sign of $\langle\cos(\theta)\rangle$ of the first few layers of water molecules is opposite that for the homogeneous and localized charge surfaces (Figure 3a,b). Moreover, the dependence of orientational ordering on the magnitude of surface charge at a given ionic strength is very different for the two types of charge distributions (Figure 3a,b). At the homogeneously charged surface (Figure 3a), the water orientation shows oscillations suggesting layering, i.e., the formation of a compact layer, up to ∼1 nm with at least 3 distinct peaks, possibly 4, followed by a "diffuse layer" exponentially decaying $\langle\cos(\theta)\rangle$. The penetration depth of this diffuse layer is found to be 0.7 nm, by fitting the $\langle\cos(\theta)\rangle$ beyond 1.2 nm to an exponential decay function (gray and pink solid fit lines fits for the 2 and 1 e/nm^2, respectively). The amplitudes of the peaks of the compact layer region are greater for the largest charge density, However, the penetration depth

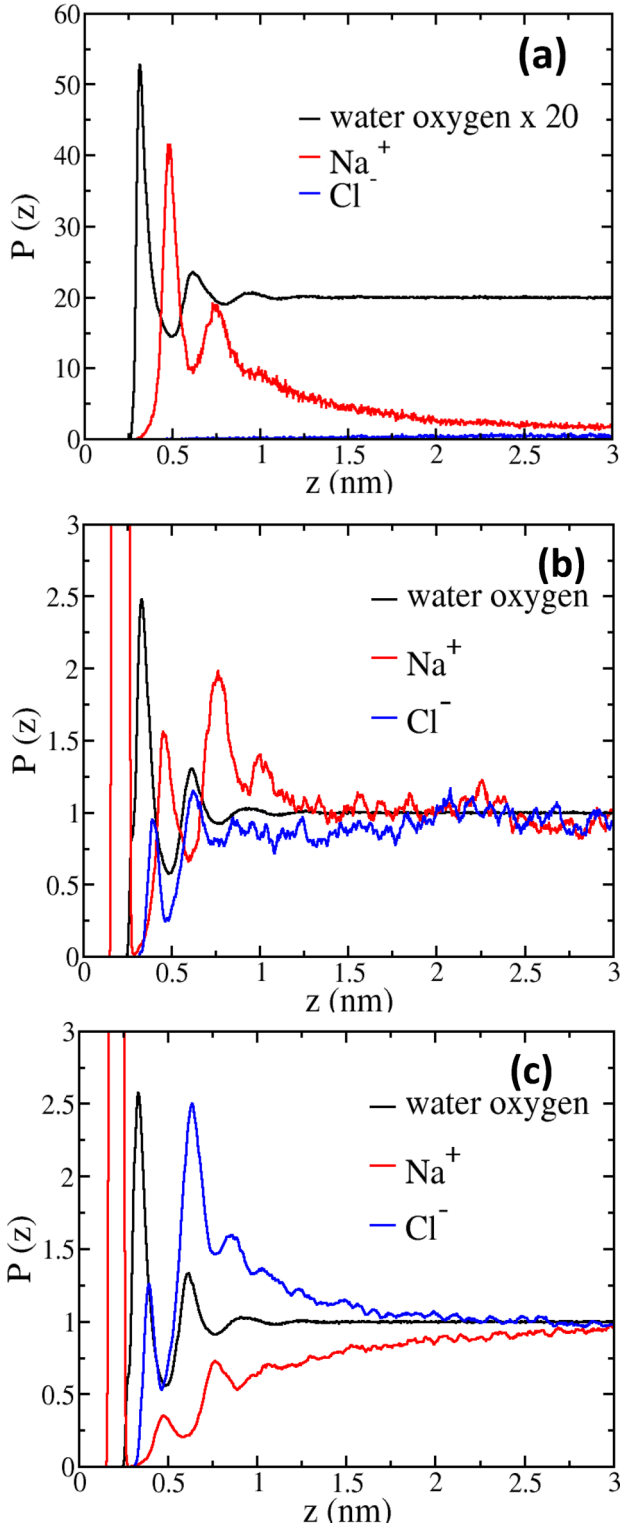

Figure 2. Density profiles of Na^+ (red), Cl^- (blue), and O of water (black) as a function of depth at the idealized charged (1 e/nm^2) surface for (a) homogeneously spread charge at 0.5 M NaCl, (b) localized charge with 0.1 M NaCl, and (c) localized charge with 0.5 M NaCl. Mass densities (kg/m^3) were rescaled to get an asymptotic (bulk) value of 1 for all the densities except where otherwise specified.

dx.doi.org/10.1021/la5011055 | Langmuir 2014, 30, 8056−8065

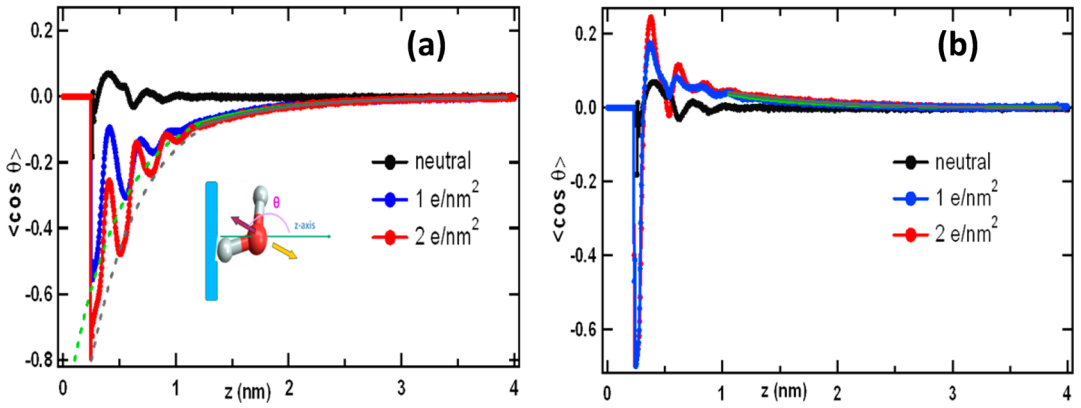

Figure 3. Effect of surface charge on the orientational ordering, $\langle\cos(\theta)\rangle$, of interfacial water at 0.5 M NaCl for surface with (a) homogeneous charge and (b) localized charge distributions. Black plot in both graphs is the density profile of oxygen when there is zero charge in surface and no ions in solution. Green dashed line: trace for compact layer for 1 e/nm^2; gray dotted line: trace for compact layer for 2 e/nm^2; green solid line: fit to exponential function for 1 e/nm^2; gray solid line: fit to exponential function for 2 e/nm^2. Inset in (a): cartoon depicting orientation for water molecules with negative $\cos(\theta)$, where θ is the angle between the purple arrow (opposite of the dipole moment) and the surface normal.

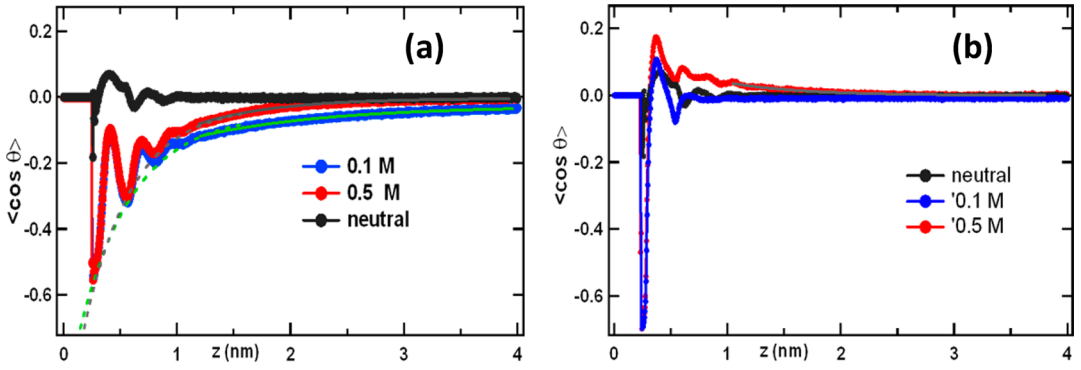

Figure 4. Effect of ionic strength on the orientation of water at zero surface charge (black curve) and constant surface charge of 1 e/nm^2 (red and blue) for (a) homogeneously spread surface charge and (b) localized charge surface. Green dashed line: trace for compact layer for 0.1 M NaCl; gray dotted line: trace for compact layer for 0.5 M salt; green solid line: fit to exponential function for 0.1 M; gray solid line: fit to exponential function for 0.5 M.

of the compact layer is similar (~0.46 nm) for both surface charge magnitudes (gray and pink dotted lines serve as guide to the eye for compact layer) (Figure 3a).

When the surface charge is localized (Figure 3b), the orientation of the first compact layer consists of water molecules oriented with their hydrogens facing the surface (Figure 3b), similar to what is seen for the case of a homogeneously distributed charge. However, the following layers are characterized by a positive $\langle\cos(\theta)\rangle$, suggesting an overall orientation with most hydrogens pointing away from the surface. This observation, along with the shoulder-like feature in the density profile of oxygen of water (Figure 1c), is evidence for the specific adsorption of Na^+ ions when charge is localized. The diffuse layer that follows the compact layer shows the same penetration depth irrespective of the surface charge magnitude (Figure 3b).

Orientational Order: Effect of Ionic Strength. The next question concerns the effect of increasing salt concentration on the orientation of interfacial water. To address this issue, we compare the orientational ordering at 0.1 and 0.5 M NaCl for the two types of surfaces with 1 e/nm^2 surface charge (Figure 4). In both cases, the first layer of water has a negative $\langle\cos(\theta)\rangle$ value, indicating that waters are oriented with their hydrogens pointing toward the negative surface. When the charge is spread (Figure 4a), increasing the ionic strength from 0.1 to 0.5 M changes the penetration depth of the diffuse layer of oriented waters from 1.1 to 0.8 nm, as obtained from exponential fits. The depth of the compact layer is comparable for the two salt concentrations (Figure 4a). In other words, at a uniformly charged surface, only the diffuse part of the interfacial region follows the Gouy−Chapman model and its dependence on ionic strength. When the charge is localized (Figure 4b), the ionic-strength dependence of the diffuse layer is more apparent. The first thin layer of water oriented with hydrogens pointing toward surface, indicated by negative $\langle\cos(\theta)\rangle$, does not change with ionic strength. For 0.1 M NaCl, in addition to the first compact layer there is no apparent diffuse layer, suggesting that the presence of an adsorbed layer of cations has completely screened the surface charge over a short distance from the surface. There is a second layer of water oriented with the hydrogen atoms pointing toward the surface, present at ~0.5 nm from the surface, which is not present in the neutral case. This small net orientation is possibly due to a residual surface charge from incomplete screening at this ionic concentration. On adding more salt (0.5 M), the positive $\langle\cos(\theta)\rangle$ associated with the second and subsequent water layers increases. Simultaneously, a diffuse layer now persists beyond the compact layer with a penetration depth of 0.65 nm, which is lower than that at the homogeneously charged surface. A possible explanation for this observation is that the adsorbed

dx.doi.org/10.1021/la5011055 | Langmuir 2014, 30, 8056−8065

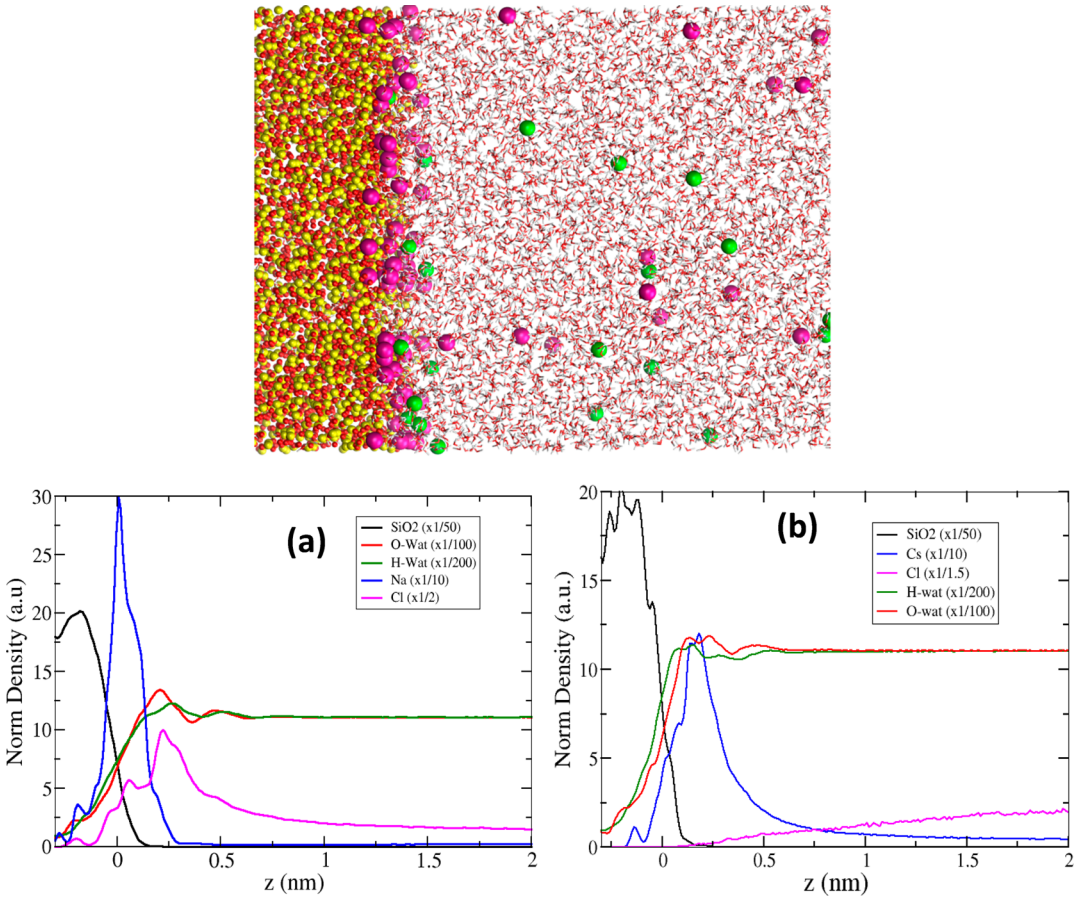

Figure 5. Density profiles of all oxygen, hydrogen, cation, chloride, and silica as a function of distance from a model silica surface with a charge density of 1.3 e/nm^2 for (a) 0.35 M NaCl and (b) 0.35 M CsCl solutions. Top left: snapshot of the am. Silica/NaCl simulation box, magenta spheres Na^+ and green spheres Cl^-. Number densities are normalized, i.e., the integral over the box length along the *z* direction returns the total number of particles (the bin size is 0.011 nm). For clarity, values are rescaled as indicated in the insets.

cations form a positive charge capacitance layer driving the waters to orient themselves with hydrogens facing away from the surface (Figure 4b). This flipping of water orientation direction has been reported theoretically and experimentally when surface charge is reversed.[19,49]

In summary, cations specifically adsorb at the negative surface only when the charge is localized (Figures 2b and 3b). As a result, the surface charge is effectively screened, reducing the net orientation of water. Interfacial water can be considered to consist of two layers: a compact layer where water orientation shows oscillations corresponding to 3-4 monolayers and a diffuse layer that closely follows Gouy−Chapman with a penetration depth sensitive to ionic strength but not the surface charge magnitude. The diffuse layer, in the case of localized negative charge, is oriented by the positive Na adsorbed layer and has a 1/e depth of 0.64 nm, smaller than depth for homogeneously charged surfaces where the orientation of water is driven by negative surface. It should be noted that the Debye length for these conditions is calculated to be 0.95 and 0.42 nm for 0.1 and 0.5 M, respectively. This means that at low concentration the depth of oriented water (1.1 nm) is close to the Debye length, while at higher concentration, depth of oriented water (0.8 nm) is greater than the Debye length. A key determinant of the structure and orientation of water at a negatively charged surface is the nature of the charge distribution, i.e., whether the charge is localized or homogeneously distributed. This factor is crucial because it impacts the process of specific adsorption, which in turn determines the degree of screening of the surface charge.

Na versus Cs at Charged Amorphous Silica Surface. As the distribution of surface charge (spread versus localized) changes the properties of interfacial water significantly, an interesting question that follows is, what type of charge distribution dependence is observed at a mineral/water interface? To address this, we carried out MD simulations using a model of an amorphous silica surface with a fixed density of SiO^- groups, corresponding to a net surface charge density of 1.3 e/nm^2. This corresponds to the charge density of silica at pH 10−11, estimated based on the fraction of deprotonated SiOH groups of the ∼4.6 SiOH groups per nm^2.[50] The simulations were performed separately for two salts: 0.35 M NaCl solution and 0.35 M CsCl, for comparison, with the same number of water molecules and silica surface. The density profiles of all the atoms in the simulation box clearly show a qualitatively different picture for the NaCl and CsCl solutions (Figure 5a,b), within 1 nm from silica surface. In the NaCl case, the density peaks for Na^+ are closer to the surface than the oxygen and hydrogen density peaks. Comparing these density profiles to those at the model charge localized surface (Figure 1b,c), it can be inferred that Na^+ ions stick to the silica surface without their hydration shells. There is also a considerable density of Cl^- ions within the 1 nm interfacial region, also similar to the picture in Figure 1b,c. In the case of CsCl, while there is a clear accumulation of Cs^+ ions near the

dx.doi.org/10.1021/la5011055 | *Langmuir* 2014, 30, 8056−8065

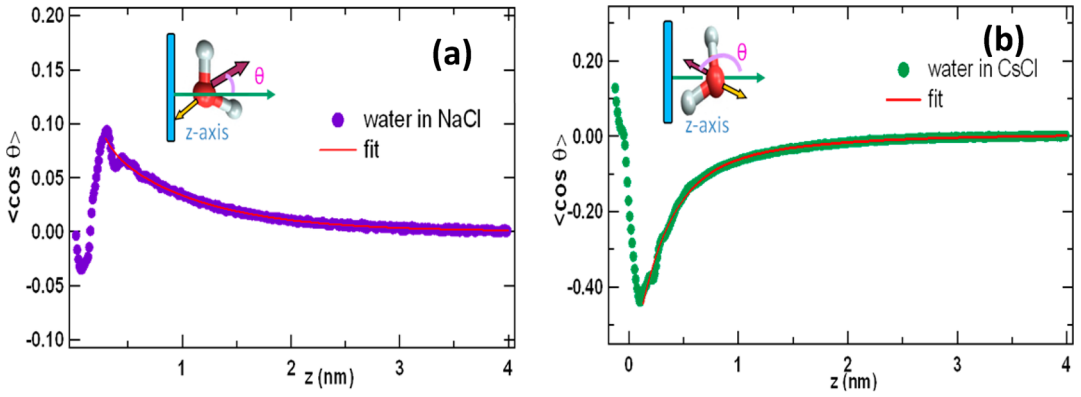

Figure 6. Orientation of water molecules, given as $\langle\cos(\theta)\rangle$, where θ is the angle between the opposite to the water dipole and the surface normal, as a function of distance from the silica surface when the electrolyte is (a) 0.35 M NaCl and (b) 0.35 M CsCl.

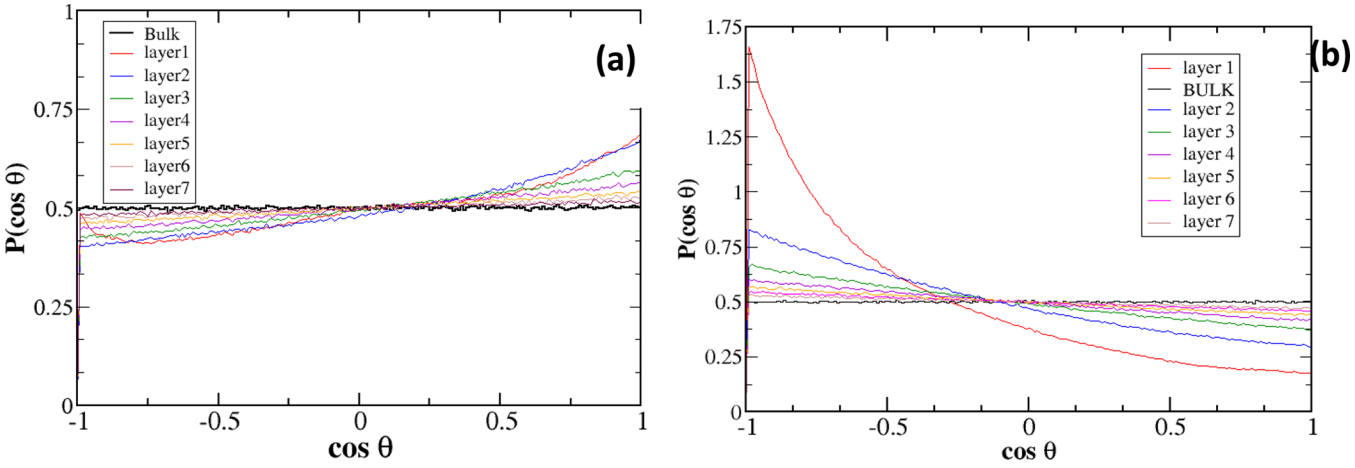

Figure 7. Layerwise distribution of water molecules having with $\cos(\theta)$ values between −1 and 1 to indicate the fraction of oriented water molecules at the amorphous silica surface for (a) 0.35 M NaCl and (b) 0.35 M CsCl.

silica surface, the hydrogens of water are closer to the surface than the Cs ions. This suggests that Cs^+ ions retain their hydration shell and do not directly adsorb to the silica surface unlike Na^+. Also, the depletion of Cl^- close to the surface resembles the situation in the homogeneously spread charge surface (Figure 1a). The significant accumulation of Na^+ within 1.2 nm is consistent with other MD simulation results that report charge inversion in silica nanochannels.[51]

Number of Adsorbed Cations. To quantify the difference in interfacial water caused by two cations at the same surface, we integrate the number of cations under the density profile peak and divide by silica surface area to determine the surface density of adsorbed cations in each case. We find that the number of Na^+ adsorbed per area of the silica surface is ∼1.6/nm^2, while for Cs^+ it is ∼1.06/nm^2. The 1.6 Na/nm^2 is in good agreement with the cation excess charge reported for the water/silica surface at pH ∼10−11, the pH regime that would have the surface charge density of 1.3 e/nm^2 as in our system.[52] According to Porus et al., at pH of 10 and 100 mM, the amount of adsorbed Na^+ is 10% higher than that of Cs^+, qualitatively consistent with our analysis.[52] The observation that Na^+ ions adsorb on silica more than Cs^+ is also supported by the SHG study by Azam et al., who report that, at high pH, the silica surface shows a greater effective pK_a value in NaCl that in CsCl, suggesting that Na^+ shows more affinity for the silica surface than Cs^+.[53] (Note: here, effective pK_a refers to the silanol acidity that is induced by different cations stabilizing the siloxide on surface sites to varying extents.)

Water Orientation at Silica Surface Na^+ versus Cs^+. If the number of cations adsorbed on the negative surface depends on the cation identity, we expect that the adsorbed cation identity would play a determining role on the orientation of water at the mineral surface.[54] In fact, the sign and magnitude of $\langle\cos(\theta)\rangle$ for water at the charged amorphous silica surface is completely different depending on whether the salt is NaCl or CsCl (Figure 6a,b). At an ionic concentration of 0.35 M, Na^+ completely screens the negative surface charge so that the first layer of water molecules is oriented with hydrogens pointed away from the surface (positive $\langle\cos(\theta)\rangle$). For both salts, $\langle\cos(\theta)\rangle$ can be fit to double-exponential decay comprising of a shallow compact layer showing oscillations up to ∼1 nm, followed by a diffuse layer. For the NaCl case, the compact layer shows positive $\langle\cos(\theta)\rangle$ with a depth of ∼0.1 nm, and the slow decaying diffuse layer has a depth of 1.1 nm. The direction of orientation of water at NaCl/silica is similar to the case of the idealized surface with localized charges (Figures 3b and 4b), indicating that Na ions have screened the negative charge of silica surface.

At the same ionic strength of 0.35 M, Cs ions do not adsorb sufficiently to screen the surface charge, since the water molecules are oriented with hydrogens facing the surface, as reflected by negative $\langle\cos(\theta)\rangle$ values. This also explains the observation of hydrogen peaks before Cs peak in the density

dx.doi.org/10.1021/la5011055 | Langmuir 2014, 30, 8056−8065

profile of Figure 6b. For the CsCl case, the compact region is deeper with a depth of 0.3 nm, while the diffuse region has a depth of 0.9 nm, comparable to NaCl case. Thus, even though the magnitude and sign of $\langle\cos(\theta)\rangle$ are different for NaCl/silica versus CsCl/silica, the interfacial depth, given by the depth of the diffuse layer, is ∼1 nm, irrespective of the cation. The observation that Na^+ ions specifically adsorb to the silica surface significant screening the negative the charge that would orient the water dipoles in the absence of the salt is in good agreement with the vSFG ultrafast dynamics and SHG results[26,28] and also with the SFG results reported by Flores et al., where the signal from the water/silica interface is perturbed more by NaCl than by CsCl.[55] A possible explanation for the difference observed between adsorption of Na^+ and Cs^+ relies on the balance between ion-surface interaction energy and the entropy loss associated with localization of the ion on the surface. Given the larger size of the nonhydrated Cs ion, the electrostatic interaction energy, which decreases with the distance between the center of the ion and surface, is not sufficient to drive desolvation and binding of Cs^+. This competition between hydration and attraction to the surface determining the location of counterions at the surface has been reported for charged clay systems.[54] In these respects, a more complex description of electrostatic interactions including the effects of polarization could potentially provide a more realistic picture of ion adsorption.[54]

Layerwise Ordering of Water at Silica Surface. We can further analyze the ordering behavior of water at the silica surface in the presence of NaCl or CsCl to quantify oriented water layers at the surface. For this, we present a layerwise distribution of the $\langle\cos(\theta)\rangle$ of water (Figure 7), where each layer corresponds to a slab with a thickness of ∼3 Å; e.g., layer 1 extends from the silica surface to ∼2.8 Å and so on. In both cases, the bulk water layer, taken ∼13 nm away from surface, shows a flat distribution, as expected for a centrosymmetric bulk water environment. Quantitatively, one can envision the extent of deviation from zero to reflect the fraction of water molecules that are oriented, i.e., the extent to which the environment is not centrosymmetric. As apparent in Figure 7, the number of oriented water molecules in the first layer at the NaCl/silica is much less than that in the first layer at the CsCl/silica interface, also supported by SFG measurements.[55] However, the direction of orientation is opposite for two cases. At the CsCl/silica interface, the second layer shows a drastic drop in the fraction of waters oriented, indicating that the orientation of the first layer of water helps in screening the negative surface charge by arranging their dipoles away from the surface. At the NaCl/silica interface (Figure 7a), the water in the first layer shows an orientation with dipoles pointing toward the surface and then a gradual layerwise decrease in the fraction of waters oriented. It is our interpretation that because Na^+ adsorbs to the surface in sufficient numbers to actually reverse the interfacial charge, the orientation of water is determined by the Na^+ layer and is opposite to what would be expected for a negative surface.

Interestingly, for both systems, by the sixth layer, i.e., ∼1.7 nm from the surface, the same percentage of water molecules shows a $\langle\cos(\theta)\rangle$ distribution different from bulk water. The percentage of oriented water is estimated as the fraction of water molecules that deviate from the bulk orientational distribution, i.e., the orientational anisotropy. For example, in the sixth layer, the percentage of water molecules with a negative $\cos(\theta)$ value is 48.4%, and 51.6% have a $\cos(\theta)$ value between 0 and +1. Thus, there is an excess, 3.2% of waters that are "oriented" with hydrogens pointed away from surface. It is this population that has a net polar order. It is remarkable that, although the first two layers of water show qualitatively and quantitatively different orientations, the depth of interface is the same for the two cations. We hypothesize that this difference results from the fact that, while at 0.35 M specific adsorption of Na^+ has reached saturation, a significant amount of Cs^+ is still in solution.

■ CONCLUSIONS

MD simulations of water with two different simplified models of charged surfaces show that the depth of the interfacial region, as intuitively defined by the distance over which water shows a net polar ordering, is mainly driven by the extent of adsorption of cations on the surface. The interface comprises of two distinct regions: a compact layer closer to the surface showing oscillations in orientation and a diffuse layer similar to that predicted by the GCS model. The diffuse layer depth not only depends on the ionic strength, as expected from EDL theories, but also is sensitive to the type of charge distribution on the surface. In the case of localized surface charge, the counterions are directly adsorbed on the charged surface and the diffuse layer does not exist. Surprisingly, with this type of interface, the addition of more ions (0.5 M NaCl) reverses the orientation of interfacial waters, i.e., increases the fraction of water with hydrogens pointing away from the surface.

On comparing the MD simulation results on amorphous silica/water interface with NaCl against CsCl, it is clear that there is specific-ion behavior, with Na^+ ions directly adsorbing at the silica surface, while Cs^+ does not directly bind to the surface but follows the GCS model. The direction of the orientation of water molecules and the length of the compact layer are different in the presence of different cations. However, the interfacial depth, given by the distance over which the diffuse region persists, is ∼1 nm, or ∼3−4 monolayers, from the negatively charged surface, irrespective of the cation. Our results thus provide a conceptual framework to describe interfacial water structure at charged surfaces, more specifically mineral, with details that the Gouy−Chapman or Gouy−Chapman−Stern theories may fail to describe. Note that the behavior observed in these simulations is peculiar of systems characterized by exposed charged groups. Several mineral interfaces, e.g. clays, contain charges localized on atoms belonging to one of the inner layers.[54] Thus, these results may not be generalizable to all mineral−water interfaces. Further interesting solvent orientational effects and hydrogen bonding properties need to be probed along the *XY* direction, at a more realistic quartz surface to reveal a complete understanding of interfacial water structure.

■ AUTHOR INFORMATION

Corresponding Author

*E-mail eborguet@temple.edu; Ph 215-2404-9696 (E.B.).

Notes

The authors declare no competing financial interest.

■ ACKNOWLEDGMENTS

The computations were performed using resources from the Temple University High-Performance Computing System purchased in part with NSF Grant MRI-R2 0958854. We are grateful for partial support (A.B. and M.L.K.) from DOE BES

Award DE FG-0212ER16333. S.D. and E.B. thank Prof. F.M Geiger for useful discussions.

REFERENCES

(1) Kasson, P. M.; Lindahl, E.; Pande, V. S. Water ordering at membrane interfaces controls fusion dynamics. *J. Am. Chem. Soc.* **2011**, *133*, 3812−3815.

(2) Levy, Y.; Onuchic, J. N. Water mediation in protein folding and molecular recognition. *Annu. Rev. Biophys. Biomol. Struct.* **2006**, *35*, 389−415.

(3) Raschke, T. M. Water structure and interactions with protein surfaces. *Curr. Opin. Struct. Biol.* **2006**, *16*, 152−159.

(4) Dove, P. M. The dissolution kinetics of quartz in sodium chloride solutions at 25° to 300° C. *Am. J. Sci.* **1994**, *294*, 665−712.

(5) Ohlin, C. A.; Villa, E. M.; Rustad, J. R.; Casey, W. H. Dissolution of insulating oxide materials at the molecular scale. *Nat. Mater.* **2011**, *9*, 11−19.

(6) Jungwirth, P.; Tobias, D. J. Ions at the air/water interface. *J. Phys. Chem. B* **2002**, *106*, 6361−6373.

(7) Zhang, R.; Somasundaran, P. Advances in adsorption of surfactants and their mixtures at solid/solution interfaces. *Adv. Colloid Interface Sci.* **2006**, *123-126*, 213−229.

(8) Narayan, S.; Muldoon, J.; Finn, M. G.; Fokin, V. V.; Kolb, H. C.; Sharpless, K. B. "On water": Unique reactivity of organic compounds in aqueous suspension. *Angew. Chem., Int. Ed.* **2005**, *44*, 3275−3279.

(9) Walther, J. H.; Jaffe, R.; Halicioglu, T.; Koumoutsakos, P. Carbon nanotubes in water: structural characteristics and energetics. *J. Phys. Chem. B* **2001**, *105*, 9980−9987.

(10) Bockris, J. O. M.; Reddy, A. K. N. *Modern Electrochemistry 2B: Electrodics in Chemistry, Engineering, Biology and Environmental Science*; Springer: Berlin, 2001; Vol. *2*.

(11) Fayer, M. D.; Levinger, N. E. Analysis of water in confined geometries and at interfaces. *Annu. Rev. Anal. Chem.* **2010**, *3*, 89−107.

(12) Gun'ko, V. M.; Turov, V. V.; Bogatyrev, V. M.; Zarko, V. I.; Leboda, R.; Goncharuk, E. V.; Novza, A. A.; Turov, A. V.; Chuiko, A. A. Unusual properties of water at hydrophilic/hydrophobic interfaces. *Adv. Colloid Interface Sci.* **2005**, *118*, 125−172.

(13) Jeffrey, G. A.; Jeffrey, G. A. *An Introduction to Hydrogen Bonding (Topics in Physical Chemistry)*; Oxford University Press: New York, 1997; Vol. *12*.

(14) Morita, A.; Hynes, J. T. A theoretical analysis of the sum frequency generation spectrum of the water surface. *Chem. Phys.* **2000**, *258*, 371−390.

(15) Townsend, R. M.; Jan, G.; Stuart, A. R. Structure of the liquid-vapor interface of water. *J. Chem. Phys.* **1985**, *82*, 4391−4392.

(16) Willard, A. P.; Reed, S. K.; Madden, P. A.; Chandler, D. Water at an electrochemical interface - a simulation study. *Faraday Discuss.* **2009**, *141*, 423−441.

(17) Gragson, D. E.; Richmond, G. L. Potential dependent alignment and hydrogen bonding of water molecules at charged air/water and CCl_4/water interfaces. *J. Am. Chem. Soc.* **1998**, *120*, 366−375.

(18) Kjellander, R.; Marcelja, S. Perturbation of hydrogen bonding in water near polar surfaces. *Chem. Phys. Lett.* **1985**, *120*, 393−396.

(19) Nihonyanagi, S.; Yamaguchi, S.; Tahara, T. Direct evidence for orientational flip-flop of water molecules at charged interfaces: A heterodyne-detected vibrational sum frequency generation study. *J. Chem. Phys.* **2009**, *130*, 204704−5.

(20) Osawa, M.; Tsushima, M.; Mogami, H.; Samjeske, G.; Yamakata, A. Structure of water at the electrified platinum/water interface: A study by surface-enhanced infrared absorption spectroscopy. *J. Phys. Chem. C* **2008**, *112*, 4248−4256.

(21) Ostroverkhov, V.; Waychunas, G. A.; Shen, Y. R. New information on water interfacial structure revealed by phase-sensitive surface spectroscopy. *Phys. Rev. Lett.* **2005**, *94*, 046102.

(22) Striolo, A. From interfacial water to macroscopic observables: A review. *Adsorpt. Sci. Technol.* **2011**, *29*, 211−258.

(23) Bard, A. J.; Faulkner, L. R. *Electrochemical Methods: Fundamentals and Applications*, 2nd ed.; John Wiley and Sons: New York, 2001.

(24) Tournassat, C.; Chapron, Y.; Leroy, P.; Bizi, M.; Boulahya, F. Comparison of molecular dynamics simulations with triple layer and modified Gouy-Chapman models in a 0.1 M NaCl-montmorillonite system. *J. Colloid Interface Sci.* **2009**, *339*, 533−541.

(25) Wang, H.; Borguet, E.; Yan, E. C. Y.; Zhang, D.; Gutow, J.; Eisenthal, K. B. Molecules at liquid and solid surfaces. *Langmuir* **1998**, *14*, 1472−1477.

(26) Eftekhari-Bafrooei, A.; Borguet, E. Effect of electric fields on the ultrafast vibrational relaxation of water at a charged solid/liquid interface as probed by vibrational sum frequency generation. *J. Phys. Chem. Lett.* **2011**, *2*, 1353−1358.

(27) Jena, K. C.; Covert, P. A.; Hore, D. K. The effect of salt on the water structure at a charged solid surface: Differentiating second- and third-order nonlinear contributions. *J. Phys. Chem. Lett.* **2011**, *2*, 1056−1061.

(28) Dewan, S.; Yeganeh, M. S.; Borguet, E. Experimental correlation between interfacial water structure and mineral reactivity. *J. Phys. Chem. Lett.* **2013**, *4*, 1977−1982.

(29) Campen, R. K.; Pymer, A. K.; Nihonyanagi, S.; Borguet, E. Linking surface potential and deprotonation in nanoporous silica: Second harmonic generation and acid/base titration. *J. Phys. Chem. C* **2010**, *114*, 18465−18473.

(30) Wang, Y.; Hodas, N. O.; Jung, Y.; Marcus, R. A. Microscopic structure and dynamics of air/water interface by computer simulations-comparison with sum-frequency generation experiments. *Phys. Chem. Chem. Phys.* **2011**, *13*, 5388−5393.

(31) Sulpizi, M.; Salanne, M.; Sprik, M.; Gaigeot, M.-P. Vibrational sum frequency generation spectroscopy of the water liquid−vapor interface from density functional theory-based molecular dynamics simulations. *J. Phys. Chem. Lett.* **2012**, *4*, 83−87.

(32) Tobias, D. J.; Hemminger, J. C. Getting specific about specific ion effects. *Science* **2008**, *319*, 1197−1198.

(33) Chyuan-Yih, L.; McCammon, J. A.; Rossky, P. J. The structure of liquid water at an extended hydrophobic surface. *J. Chem. Phys.* **1984**, *80*, 4448−4455.

(34) Giovambattista, N.; Debenedetti, P. G.; Rossky, P. J. Effect of surface polarity on water contact angle and interfacial hydration structure. *J. Phys. Chem. B* **2007**, *111*, 9581−9587.

(35) Argyris, D.; Tummala, N. R.; Striolo, A.; Cole, D. R. Molecular structure and dynamics in thin water films at the silica and graphite surfaces. *J. Phys. Chem. C* **2008**, *112*, 13587−13599.

(36) Zhang, H.; Hassanali, A. A.; Shin, Y. K.; Knight, C.; Singer, S. J. The water-amorphous silica interface: Analysis of the Stern layer and surface conduction. *J. Chem. Phys.* **2011**, *134*, 024705−13.

(37) Argyris, D.; Cole, D. R.; Striolo, A. Ion-specific effects under confinement: The role of interfacial water. *ACS Nano* **2010**, *4*, 2035−2042.

(38) Ho, T. A.; Argyris, D.; Cole, D. R.; Striolo, A. Aqueous NaCl and CsCl solutions confined in crystalline slit-shaped silica nanopores of varying degree of protonation. *Langmuir* **2012**, *28*, 1256−1266.

(39) Marry, V.; Rotenberg, B.; Turq, P. Structure and dynamics of water at a clay surface from molecular dynamics simulation. *Phys. Chem. Chem. Phys.* **2008**, *10*, 4802−4813.

(40) Mackerell, A. D. Empirical force fields for biological macromolecules: Overview and issues. *J. Comput. Chem.* **2004**, *25*, 1584−1604.

(41) MacKerell, A. D.; Banavali, N. K. All-atom empirical force field for nucleic acids: II. Application to molecular dynamics simulations of DNA and RNA in solution. *J. Comput. Chem.* **2000**, *21*, 105−120.

(42) Darve, E.; Rodriguez-Gomez, D.; Pohorille, A. Adaptive biasing force method for scalar and vector free energy calculations. *J. Chem. Phys.* **2008**, *128*, 144120.

(43) Jorgensen, W. L.; Chandrasekhar, J.; Madura, J. D.; Impey, R. W.; Klein, M. L. Comparison of simple potential functions for simulating liquid water. *J. Chem. Phys.* **1983**, *79*, 926−935.

(44) Essmann, U.; Perera, L.; Berkowitz, M. L.; Darden, T.; Lee, H.; Pedersen, L. G. A smooth particle mesh Ewald method. *J. Chem. Phys.* **1995**, *103*, 8577−8593.

(45) Phillips, J. C.; Braun, R.; Wang, W.; Gumbart, J.; Tajkhorshid, E.; Villa, E.; Chipot, C.; Skeel, R. D.; Kalé, L.; Schulten, K. Scalable molecular dynamics with NAMD. *J. Comput. Chem.* **2005**, *26*, 1781−1802.
(46) Cruz-Chu, E. R.; Aksimentiev, A.; Schulten, K. Water-silica force field for simulating nanodevices. *J. Phys. Chem. B* **2006**, *110*, 21497−21508.
(47) Lee, S. H.; Rossky, P. J. A comparison of the structure and dynamics of liquid water at hydrophobic and hydrophilic surfaces - a molecular dynamics simulation study. *J. Chem. Phys.* **1994**, *100*, 3334−3345.
(48) Xu, D.; Leng, Y.; Chen, Y.; Li, D. Water structures near charged (100) and (111) silicon surfaces. *Appl. Phys. Lett.* **2009**, *94*, 201901−3.
(49) Schweighofer, K. J.; Essmann, U.; Berkowitz, M. Structure and dynamics of water in the presence of charged surfactant monolayers at the water/CCl_4 interface. A molecular dynamics study. *J. Phys. Chem. B* **1997**, *101*, 10775−10780.
(50) Zhuravlev, L. T. The surface chemistry of amorphous silica. Zhuravlev model. *Colloids Surf., A* **2000**, *173*, 1−38.
(51) Lorenz, C. D.; Crozier, P. S.; Anderson, J. A.; Travesset, A. Molecular dynamics of ionic transport and electrokinetic effects in realistic silica channels. *J. Phys. Chem. C* **2008**, *112*, 10222−10232.
(52) Porus, M.; Labbez, C.; Maroni, P.; Borkovec, M. Adsorption of monovalent and divalent cations on planar water-silica interfaces studied by optical reflectivity and Monte Carlo simulations. *J. Chem. Phys.* **2011**, *135*, 064701-9.
(53) Azam, M. S.; Weeraman, C. N.; Gibbs-Davis, J. M. Specific cation effects on the bimodal acid/base behavior of the silica/water interface. *J. Phys. Chem. Lett.* **2012**, *3*, 1269−1274.
(54) Botan, A.; Marry, V.; Rotenberg, B.; Turq, P.; Noetinger, B. How electrostatics influences hydrodynamic boundary conditions: Poiseuille and electro-osmostic flows in clay nanopores. *J. Phys. Chem. C* **2013**, *117*, 978−985.
(55) Flores, S. C.; Kherb, J.; Konelick, N.; Chen, X.; Cremer, P. S. The effects of Hofmeister cations at negatively charged hydrophilic surfaces. *J. Phys. Chem. C* **2012**, *116*, 5730−5734.